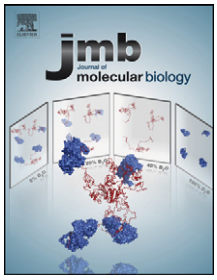

Shifting Fitness and Epistatic Landscapes Reflect Trade-offs along an Evolutionary Pathway

Barrett Steinberg and Marc Ostermeier

Department of Chemical and Biomolecular Engineering, *Johns Hopkins University, 3400 N. Charles St., Baltimore, MD 21218, USA*

Correspondence to Marc Ostermeier: *oster@jhu.edu.*
http://dx.doi.org/10.1016/j.jmb.2016.04.033
Edited by Dan Tawfik

Abstract

Nature repurposes proteins via evolutionary processes. Such adaptation can come at the expense of the original protein's function, which is a trade-off of adaptation. We sought to examine other potential adaptive trade-offs. We measured the effect on ampicillin resistance of ~12,500 unique single amino acid mutants of the *TEM-1*, *TEM-17*, *TEM-19*, and *TEM*-15 β-lactamase alleles, which constitute an adaptive path in the evolution of cefotaxime resistance. These protein fitness landscapes were compared and used to calculate epistatic interactions between these mutations and the two mutations in the pathway (E104K and G238S). This series of protein fitness landscapes provides a systematic, quantitative description of pairwise/tertiary intragenic epistasis involving adaptive mutations. We find that the frequency of mutations exhibiting epistasis increases along the evolutionary pathway. Adaptation moves the protein to a region in the fitness landscape characterized by decreased mutational robustness and increased ruggedness, as measured by fitness effects of mutations and epistatic interactions for TEM-1's original function. This movement to such a "fitness territory" has evolutionary consequences and is an important adaptive trade-off and cost of adaptation. Our systematic study provides detailed insight into the relationships between mutation, protein structure, protein stability, and epistasis and quantitatively depicts the different costs inherent in the evolution of new functions.

Introduction

Proteins often evolve to serve new roles. Such repurposing can come at the expense of the original function, which is one type of adaptive trade-off. For instance, different beta-lactamases (β-lactamases) provide different levels of resistance to beta-lactam (β-lactam) antibiotics [1]. Selective pressure for resistance to one class of β-lactam may decrease resistance to a second class. Because selective pressures can change over time, the selective history and evolutionary pathways of protein function may be complex [2,3]. When selective pressure is removed for an original function, alleles compromised in this function may become fixed in a population. Although such an event offers new evolutionary pathways for evolution to follow [4–6], it will close off other pathways available to the original allele. If the new "fitness territory" surrounding the adaptive allele is disadvantageous compared to that surrounding the original allele (i.e., beneficial mutations do not result in equivalent high fitness values, and other mutations tend to have more negative effect and result in epistatic effects producing rugged landscapes), this territorial disadvantage would be another type of adaptive trade-off. Quantitative and mechanistic understanding of all types of adaptive trade-offs is important for understanding evolutionary dynamics and outcomes. However, we lack an extensive, systematic study of changes in the fitness landscape surrounding a protein along an adaptive pathway and the extent and types of trade-offs that resulted. To better understand the trade-offs inherent in adaptation, we used protein fitness landscapes to extensively quantify the effects of adaptation on the prevalence of epistasis and how the fitness territory after adaptation differs from that before the accumulation of adaptive mutations.

The advent of deep sequencing has provided the ability for extensive studies of the effect of mutation on function and fitness for a single gene or protein [7,8]. Protein fitness landscapes provide a description of the effects of mutation on protein function or

the phenotype they provide. Most studies of protein fitness landscapes have focused on the effects of single mutations in a set genetic background, characterizing only the first possible evolutionary steps from a given allele. However, the coupled effects of mutations (i.e., epistasis) give rise to rugged landscapes, making the effect of multiple mutations difficult to predict from the effects of individual mutations [9–14]. Intragenic epistasis is believed to be enriched during adaptive evolution [14–17], but the evidence for this enrichment mostly comes from epistatic interactions between adaptive mutations or through homolog comparisons rather than a systematic study of epistasis throughout the protein along an adaptive pathway. The few large-scale studies of protein epistatic landscapes [18–23] were not designed to globally address epistasis in the context of adaptive mutations and have been limited to pairwise epistasis. With one exception [22], these studies have not examined mutations throughout an entire protein in a physiological setting. Other studies [24] relied on statistical inference of epistasis, which is subject to bias [25]. To best capture the relationships between adaptation, epistasis, and trade-offs, physiological fitness landscapes of full-length genes involving a series of alleles along an evolutionary pathway must be analyzed and compared. Here, using the *TEM-1* β-lactamase gene, we examine how protein fitness landscapes change with respect to the original function as adaptive mutations for a new function accumulate. We also investigate how the prevalence and types of epistasis change along an evolutionary pathway.

TEM-1 is highly optimized to provide penicillin resistance to bacteria but has nearly no ability to confer cefotaxime resistance. *TEM-17* (E104K), *TEM-19* (G238S), and *TEM*-15 (E104K/G238S) are clinically isolated alleles of *TEM-1* with the indicated mutations [26]. These mutations confer increased cefotaxime resistance and exhibit positive epistasis. E104K and G238S individually confer four- and eightfold increases in cefotaxime resistance, respectively, but when combined, they confer a 128-fold increase [27]. Improved resistance results from active site changes that synergistically increase catalytic activity on cefotaxime, but this adaptation comes at the expense of penicillinase activity and thermodynamic stability [28]. In particular, the G238S mutation causes the largest increase in cefotaximase activity, the largest decrease in penicillinase activity, and the largest decrease in stability ($\Delta\Delta G = -1.94$ kcal/mol) [28]. Whether E104K is slightly destabilizing [28] or slightly stabilizing [29] is uncertain, but there is agreement that the combination of G238S and E104K is approximately additive in terms of their effect on stability [28,29].

Since TEM-1 is highly specialized for penicillin hydrolysis, these adaptive mutations for cefotaxime resistance expose the allele to risk for loss in the capacity to provide resistance to penicillins such as ampicillin (Amp). For example, the G238S mutation reduces the minimum inhibitory concentration (MIC) for Amp by fourfold and reduces the k_{cat}/K_m for Amp hydrolysis by 25-fold [30]. Here, we quantify how the protein fitness landscape for Amp resistance changes along the evolutionary pathway from TEM-1 to TEM-15. Since either mutation can occur first in the evolutionary pathway to TEM-15 [31], we characterized the fitness landscapes along both possible evolutionary trajectories.

Fitness conferred by antibiotic-resistant alleles can be measured through growth competition experiments in the presence of the antibiotic; however, the fitness values depend greatly on the concentration of antibiotic used, and the method cannot distinguish fitness differences among alleles conferring antibiotic resistance far above or far below the level of resistance required for growth [32]. We skirt these limitations by measuring the effect of mutations on TEM-1's ability to confer Amp resistance using a synthetic-biology-based method that quantifies the protein's underlying fitness landscape and thus its intrinsic evolutionary potential with respect to its primary cellular function— to confer antibiotic resistance [33]. This method combines high-throughput, site-directed mutagenesis [34], a band-pass genetic circuit to partition alleles based on fitness [35], and deep sequencing to assign fitness values [33] (Supplementary Fig. S1). Although the resulting protein fitness landscape is the major determinant of an organismal fitness landscape for growth of the bacteria in the presence of the antibiotic [22], the two types of landscapes are not equivalent. However, unlike most previous large-scale studies of protein epistatic landscapes, our landscape is determined in a physiological setting and includes a mutation's effect on protein-specific activity, protein cellular abundance, and potentially other factors arising from the native cellular context. Although synonymous mutations can have small fitness effects in *TEM-1* [33], here we average the effect of synonymous mutations and measure protein fitnesses.

Results and Discussion

Fitness measurements

Our protein fitness measurements quantify the ability of the protein to provide the bacteria with resistance to the β-lactam antibiotic, much like a MIC does. Although our fitness measurements linearly correlate with the MIC [35], our measurements are technically not a MIC. We use a synthetic gene circuit that makes the bacteria behave like a band-pass filter for β-lactam hydrolysis activity. We designed this gene circuit such that sublethal levels of β-lactam

antibiotics (such as Amp and cefotaxime) cause the induction of the *tetC* gene, which provides tetracycline resistance. If the total cellular β-lactamase activity is too high relative to the β-lactam concentration, the bacteria cannot grow in the presence of tetracycline. Conversely, if the total cellular β-lactamase activity is too low relative to the β-lactam concentration, the bacteria cannot grow due to the β-lactam antibiotic. When band-pass bacteria containing a β-lactamase allele are plated in the presence of tetracycline, growth requires a particular narrow concentration range of the β-lactam antibiotic. To measure the fitness effects of mutations, we transform the library of β-lactamase alleles into the band-pass bacteria and plate them on a series of plates containing tetracycline and different concentrations of the β-lactam (Supplementary Fig. S1). This divides the library into sublibraries based on the bacteria's ability to degrade the β-lactam. We next perform deep sequencing on the β-lactamase genes on the plates and count how many times each allele appears on each plate. We then calculate the midpoint β-lactam concentration at which the allele appears most frequently (this concentration is roughly ¼ of the MIC [35]). We normalize this to the midpoint concentration at which the wild-type TEM-1 β-lactamase allele is found most often. This normalized value is the protein fitness. More details can be found in Firnberg *et al.* [33] and in the Materials and Methods.

Fitness landscapes along an evolutionary pathway

Our previous study quantified the effect on fitness (with respect to Amp resistance) of 95.6% (5212/5453) of the possible single amino acid substitutions in the TEM-1 protein [33]. Here, we quantified the fitness effects on Amp resistance of 39% of all mutations in TEM-17, 50% of all mutations in TEM-19, and 45% of all mutations in TEM-15 using the same approach (Fig. 1). As expected, based on previous MIC experiments with these alleles [27], G238S caused the greater reduction in fitness, which could be somewhat ameliorated by the E104K mutation. Fitness values relative to that of TEM-1 were 0.54 ± 0.05 (TEM-17), 0.22 ± 0.02 (TEM-19), and 0.29 ± 0.03 (TEM-15). Strikingly, a mutation's effect on TEM-15 is, in general, much more deleterious than would be predicted based on the mutation's effect on TEM-1 (Fig. 1). The mutation with the median effect in TEM-1 caused a 47% loss in fitness, whereas the same in TEM-15 caused a 66% loss (Fig. 2). Thus, the combination of these two mutations (E014K and G238S), which synergistically increases cefotaxime resistance, preferentially makes the effect of other

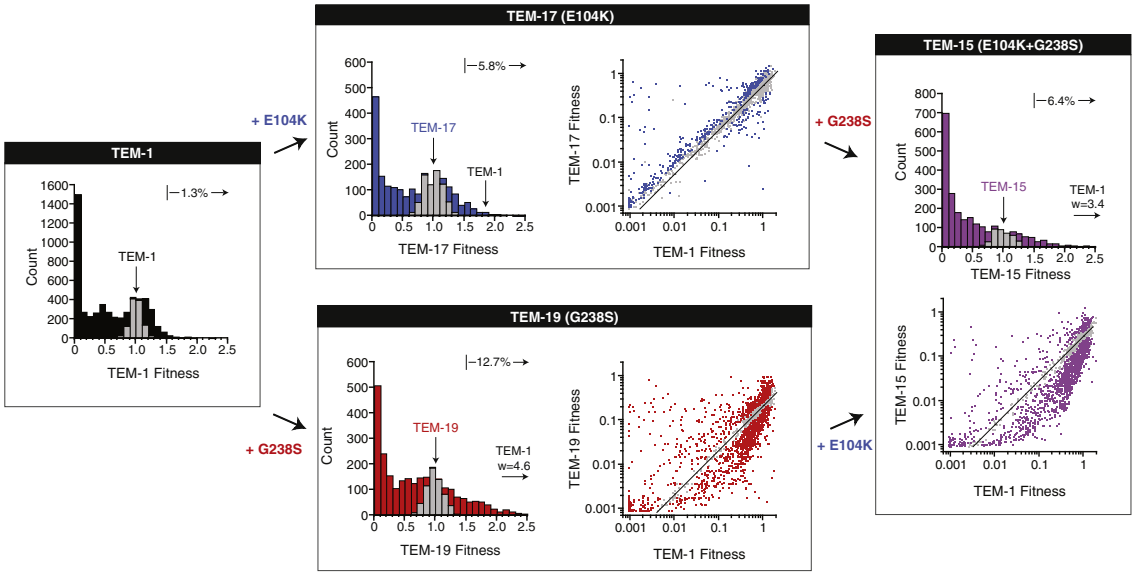

Fig. 1. Fitness landscapes along an evolutionary pathway. The gain of the adaptive mutations (E104K or G238S) for cefotaxime resistance is indicated, along with the distribution of fitness effects on Amp resistance in that context. Histograms display fitness values relative to the particular allele being characterized, with gray bars indicating fitness measurements that cannot be statistically distinguished from that of the non-mutated allele. The relative fitness of TEM-1 is indicated, along with the percent of mutants with fitness values >50% above that of the genetic background. Scatter plots show fitness values relative to TEM-1 and illustrate how well the effect of the mutation on TEM-1 can predict the effect of the mutation on the indicated allele. The lines indicate the expected value assuming no epistasis. In the scatter plots, color indicates significant (colored points) and non-significant (gray points) differences in the mutations' fitness effects in the two genetic backgrounds. Supplementary Data S1 tabulates all fitness values.

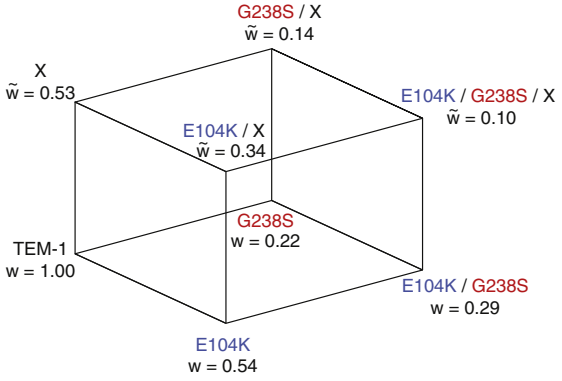

Fig. 2. The median effect of mutations on protein fitness. The cube represents the eight possible combinations of mutations E104K, G238S, and a third mutation X. Fitness values listed are for discrete values for the bottom face of the cube and median values for the top face of the cube.

mutations more deleterious for Amp resistance. This negative effect is an adaptive trade-off that primarily arises from the effects of the G238S mutation. A mutation's effect on TEM-1 was much more predictive of the mutation's effect on TEM-17 than on TEM-19. The percentage of mutations with effects statistically different than predicted was 24% and 47% for TEM-17 and TEM-19, respectively. The higher predictability of a mutation's effect in TEM-17 might be anticipated based on TEM-17's marginal effect on protein stability. On average, a mutation's effect on TEM-17 was slightly less deleterious than the mutation's effect on TEM-1 (Fig. 1). The median fitness decrease was 47% for TEM-1 but only 37% for TEM-17 (Fig. 2). This difference could reflect E104K's proposed role as a weak global suppressor mutation [36], although the difference could also result from a slight underestimation of the fitness of TEM-17. The high frequency of beneficial mutations in TEM-19 is striking (12.7% of all mutations improve fitness >50% relative to TEM-19). This finding illustrates the prevalence of compensatory mutations in the context of deleterious mutations, although these compensatory mutations do not fully restore Amp resistance to TEM-1-levels. By compensatory mutation, we mean any mutation that compensates for the negative effect of G238S, regardless of the mutation's effect in TEM-1. This protein resilience can be thought of as a corollary of the law of diminishing returns (i.e., the further the system is from an optimum, the more common the beneficial mutations). The compensatory mutations are preferentially drawn from mutations with small effects on TEM-1 fitness. In contrast, G238S and especially the combination of E104K and G238S tend to magnify the negative effects of deleterious mutations, which may be quantified by calculating the epistasis between sets of mutations.

Epistatic landscapes along an evolutionary pathway

In this study, we define epistasis as occurring when the effect of two or more mutations does not equal the product of their individual effects. Pairwise epistasis between mutation A conferring fitness w_A and mutation B conferring fitness w_B is defined as:

$$\varepsilon_{A\bullet B} = \log_{10}\left(\frac{w_{AB}w_o}{w_A w_B}\right) \quad (1)$$

in which w_o is the wild-type fitness and w_{AB} is the fitness conferred by having mutations A and B together [37]. Generalizing for epistasis of order N with mutations i,j,k…n:

$$\varepsilon_{ijk\ldots n} = \log_{10}\left(\frac{w_{ijk\ldots n}{w_o}^{N-1}}{\prod_i^n w_i}\right) \quad (2)$$

Thus, tertiary epistasis between mutations A, B, and X is

$$\varepsilon_{A\bullet B\bullet X} = \log_{10}\left(\frac{w_{ABX}{w_o}^2}{w_X w_A w_B}\right) \quad (3)$$

Tertiary epistasis can also be calculated by summing the appropriate pairwise epistasis terms

$$\begin{aligned}\varepsilon_{A\bullet B\bullet X} &= \varepsilon_{A\bullet B} + \varepsilon_{B\bullet X} + \varepsilon_{A\bullet X|B} = \varepsilon_{A\bullet B} + \varepsilon_{A\bullet X} + \varepsilon_{B\bullet X|A} \\ &= \varepsilon_{A\bullet X} + \varepsilon_{B\bullet X} + \varepsilon_{A\bullet B|X}\end{aligned} \quad (4)$$

in which $\varepsilon_{i\bullet j|k}$ refers to the pairwise epistasis between i and j in the context of allele containing mutation k. Thus, epistasis effects among E104K, G238S, and a third mutation (X), can be characterized by six pairwise epistasis terms and one tertiary epistasis term.

Figure 3 shows these seven epistatic landscapes. In our analysis, we only include epistasis values for which w_X (the fitness of TEM-1 containing mutation X) is greater than 0.02 to avoid an artifactual increase in epistasis values due to the lower limit in measuring fitness. The trends observed are opposite to or distinct from the small bias expected due to the artifactual phenomena of regression to the mean [38]. Significant epistasis involving the E104K and G238S mutations is apparent, and the extent of mutations exhibiting epistasis increases along the pathway. E104K and G238S exhibit positive epistasis (pairwise epistasis $\varepsilon_{E104K\bullet G238S} = 0.40 \pm 0.06$). This epistasis is 33% less than that previously observed with cefotaxime ($\varepsilon_{E104K\bullet G238S} = 0.60$), although the cefotaxime epistasis value is calculated from fitness values determined from low-resolution MIC assays in twofold increments [27]. The extent and magnitude of pairwise epistasis involving G238S

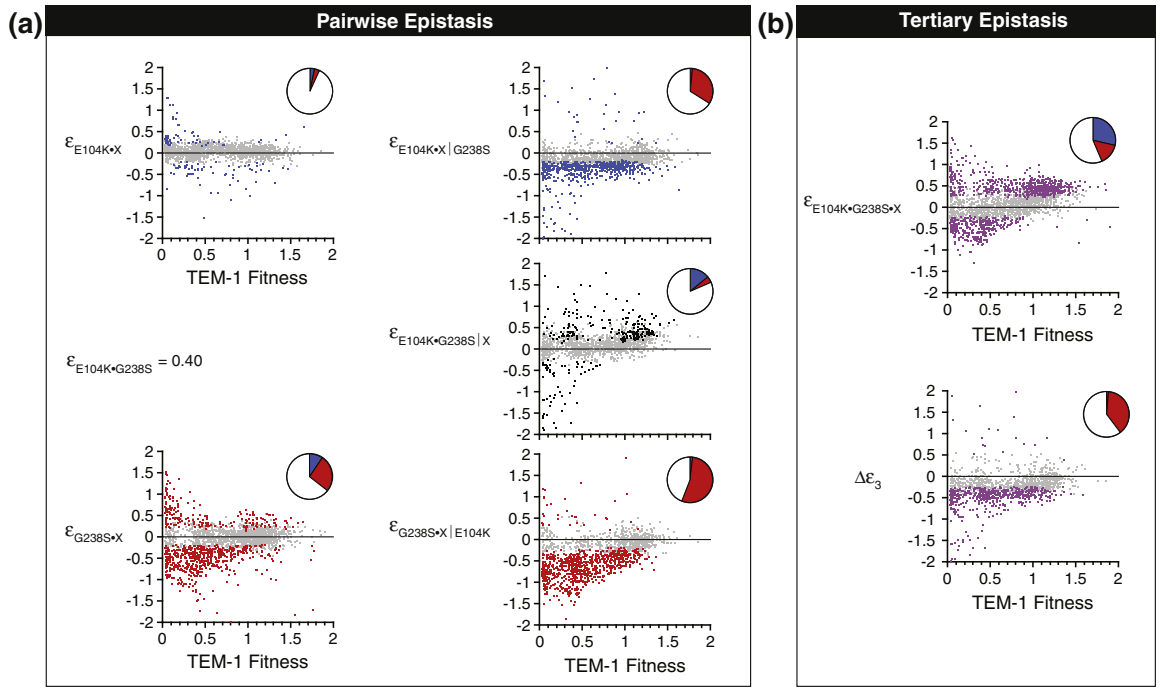

Fig. 3. Distribution of pairwise and tertiary epistasis values along an evolutionary pathway. (a) The distribution of the six possible pairwise epistasis values between two common mutations (E104K and G238S) and a third mutation (X) is shown as a function of the effect of mutation X in TEM-1. (b) Tertiary epistasis ($\varepsilon_{E014K•G238S•X}$) and the effect of adding a third mutation on the epistasis ($\Delta\varepsilon_3$) are shown as a function of the effect of mutation X on TEM-1. In the scatter plots, color indicates significant (colored points) and non-significant (gray points) epistatic effects of mutations. Pie graphs indicate the portion of alleles exhibiting positive epistasis (blue), negative epistasis (red), or no epistasis (white). Scatter plots exclude a very small number of alleles that exhibited epistasis values >2 or <-2. Supplementary Data S1 tabulates all epistasis values.

are much greater than that involving E104K (Fig. 3a). $\varepsilon_{G238S•X}$ tends toward negative epistasis values as w_X decreases, whereas $\varepsilon_{E104K•X}$ is largely independent of w_X. In other words, when mutation X has a large negative effect on the fitness of TEM-1, its effect tends to be even more negative in the context of G238S, a destabilizing mutation. This result, like those of previous studies [5,14,19,21], fits the threshold robustness model describing protein fitness landscapes [5,39,40]. This model posits a stability margin that buffers the effect of destabilizing mutations. In the cell, chaperones can also provide a buffer against the destabilizing effects of mutations by compensating for the mutation's negative effect on protein abundance [4,33]. However, once that stability margin is exhausted, the deleterious effects of destabilizing mutations are fully realized, resulting in a landscape that is inherently dominated by negative epistasis.

Although this model fits for $\varepsilon_{G238S•X}$ when considering nearly neutral and moderately deleterious mutations, the model begins to break down when considering mutations with a severe effect on TEM-1 fitness ($w_X < 0.2$), which are equally likely to exhibit positive or negative epistasis (Supplementary Fig. S2). The reason for the breakdown of the model may lie with the origin of the deleterious effects. Mutations with a severe effect on TEM-1 fitness ($w_X = \sim 0.05$) are deleterious primarily due to the mutation's effects on specific catalytic activity instead of effects on protein abundance [33]. Thus, such mutations may not necessarily erode the stability buffer as significantly. Alternatively, positive epistasis with G238S may arise from mutations that decrease stability in the same region of the protein as G238S does. Thus, positive epistasis may manifest if G238 and the mutated residue have a local stabilization interaction whose energy is lost by mutation of either position. Regardless, G238S (but not E104K) possesses the potential to either exacerbate or mitigate severely deleterious mutations, suggesting that severely destabilizing mutations move a protein into an area of the protein fitness landscape with more rugged local topography.

From the distributions of Fig. 3, one can visualize how the tertiary epistasis is composed of the sum of three pairwise epistasis values according to Eq (4). This is seen most easily by summing $\varepsilon_{E104K•G238S}$, $\varepsilon_{E104K•X}$, and $\varepsilon_{G238S•X|E104K}$. Since E104K and X exhibit little epistasis and $\varepsilon_{E104K•G238S} = +0.40$, the tertiary epistasis distribution can be seen to approximate that of $\varepsilon_{G238S•X|E104K}$ shifted up about 0.40

(Fig. 3). Thus, $\varepsilon_{G238S\bullet X|E104K}$ is the pairwise epistasis term that best predicts the shape of the distribution of tertiary epistasis values (Supplementary Fig. S3). Neutral-to-beneficial mutations in TEM-1 tend not to disrupt the positive epistasis between E104K and G238S, as can be seen by the significant tertiary epistasis values for such mutations hovering around +0.4, which is the value of $\varepsilon_{E104K\bullet G238S}$ (Fig. 3b).

Among three mutations, the amount by which a third mutation changes the epistasis is the same regardless of which mutation is considered the third mutation, as can be seen by this manipulation of Eq (4):

$$\Delta\varepsilon_3 = \varepsilon_{A\bullet B|X} - \varepsilon_{A\bullet B} = \varepsilon_{A\bullet X|B} - \varepsilon_{A\bullet X} = \varepsilon_{B\bullet X|A} - \varepsilon_{B\bullet X} \qquad (5)$$

The term $\Delta\varepsilon_3$ is the change in epistasis upon adding a third mutation. The terms $\varepsilon_{A\bullet B\bullet X}$ and $\Delta\varepsilon_3$ reflect different aspects of tertiary epistasis. Although $\varepsilon_{A\bullet B\bullet X}$ provides a measure of the epistasis involving the three residues according to Eq (3), it cannot distinguish between tertiary epistasis originating solely between two mutations and that originating in the complex interaction between all three mutations. The term $\Delta\varepsilon_3$ provides a measure of non-additive fitness effects manifesting from the three mutations collectively and better represents higher-order epistatic effects. This term is the same as the net epistatic deviation of a tertiary interaction as defined by Da Silva *et al.* [41]. They defined the net epistatic deviation as the difference between the tertiary epistasis $\varepsilon_{A\bullet B\bullet X}$ and the sum of the pairwise epistasis terms $\varepsilon_{A\bullet X}$, $\varepsilon_{B\bullet X}$, and $\varepsilon_{A\bullet B}$. Thus, $\Delta\varepsilon_3$ can be understood to be the portion of the tertiary epistasis that cannot be accounted for by the net effect of the three pairwise epistasis terms.

In our study of TEM-1, $\Delta\varepsilon_3$ reflects how mutation X influences the positive pairwise epistasis between E104K and G238S (Fig. 3b). On average, the effect is negative (median $\Delta\varepsilon_3 = -0.24$) but not enough to completely erase the positive interaction between E104K and G238S, which is why the tertiary epistasis is positive on average (median $\varepsilon_{E104K\bullet G238S\bullet X} = 0.17$). The results indicate that the positive epistasis between E104K and G238S is fragile and easily compromised by many mutations. This fragility is why the fitness effects of mutations in TEM-15 are much more deleterious than expected (Fig. 1). Due to symmetry in Eq (5), the average effect of G238S on the epistasis between E104K and X is equivalently negative, as is the effect of E104K on the epistasis between G238S and X. The term $\Delta\varepsilon_3$ is significantly negative for 38% but significantly positive for only 1.5% of all triple mutants (Fig. 3). The median $\Delta\varepsilon_3$ value for a position in the protein is nearly always negative. Thus, despite a trend toward positive tertiary epistasis values, the E104K and G238S mutations of TEM-15 brought the protein to a more precarious region of sequence space (i.e., fitness territory), in which beneficial mutations in TEM-15 do not increase fitness to the levels beneficial mutations in TEM-1 did, and a mutation's effect tends to be more negative than expected based on the mutation's effect in TEM-1, TEM-17, or TEM-19. The protein fitness landscape around TEM-15 has much steeper drop-offs in fitness than the landscape around TEM-1.

A cost of the adaptive mutations for cefotaxime is this decreased mutational robustness. We term this evolutionary exchange in landscape topology a "fitness territory" trade-off. Although this cost is illustrated here with the original function (Amp resistance), this topography likely extends to the evolved function (cefotaxime resistance) and perhaps other functions as well. We measured the fitness effects of mutations on TEM-15 for cefotaxime fitness and in general found that mutations reduced cefotaxime fitness as much or more than they reduced Amp fitness (Fig. 4). The median fitness in the presence of Amp of single mutants of TEM-15 was 0.34, relative to the fitness of TEM-15, while for cefotaxime, this value was 0.20. In contrast, the median fitness of single mutants of TEM-1 in the presence of Amp was 0.53, indicating smaller fitness declines around TEM-1. Most mutations in TEM-15 produced similar fitness effects for both antibiotics ($R^2 = 0.73$), especially for mutations causing a fitness <1.0 ($R^2 = 0.8$). This positive correlation is in contrast to the negative correlation between Amp and cefotaxime resistance among 32 alleles of TEM-1 having different combinations of five adaptive mutations for cefotaxime resistance [42]. Our result suggests that most mutations realize their effects

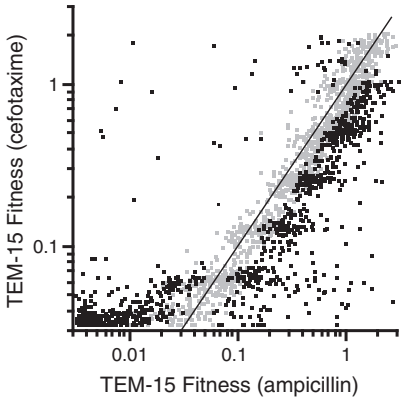

Fig. 4. Correlation between a mutation's effect on cefotaxime resistance and the effect on Amp resistance for TEM-15. Fitness values are normalized to that of TEM-15. Color indicates significant (black points) and non-significant (gray points) differences in the mutations' fitness effects in the two environments. The line is y = x. Fitness values for cefotaxime resistance cannot be measured below a value of about 0.03 - 0.04, which represents the level of resistance of cells lacking a TEM-15 gene. This accounts for the deviation from the line y = x seen at the bottom left of the graph.

through changes in protein properties common to both substrates (e.g., stability). Thus, the new fitness territory may offer less potential for evolving new resistance in general, as new mutations are less likely to both improve catalytic activity and not further erode the stability of the protein.

Evolution has mechanisms to mitigate these costs: global compensatory mutations. In TEM β-lactamases, the most well-known mutation of this type is M182T. M182T is a stabilizing mutation [28] that is found clinically in resistant alleles to a wide variety of β-lactamase substrates and inhibitors but never appears alone [43]. In most directed evolution experiments for increased resistance to cefotaxime, M182T appears after G238S [44–49]. M182T-induced stabilization has been shown to have compensatory effects for a wide variety of mutations for amoxicillin resistance [22]. Based on this information, M182T would be expected to move TEM-15 away from a precarious territory of the landscape to an area that is surrounded by higher ground with less steep drop-offs.

Structural map of epistasis

We next examined the relationship between epistasis and protein structure. G238S is 23.8% surface exposed. Mutations within 9 Å of G238S were significantly biased toward exhibiting positive pairwise epistasis with G238S (Fig. 5a) and positive tertiary epistasis (Fig. 5b), perhaps because proximal mutations cooperatively contribute toward protein stability. Assuming the null hypothesis that positive and negative epistasis are equally probable near G238, the probability of observing biases at least this severe by chance were $<1.8 \times 10^{-5}$ and $<1.0 \times 10^{-6}$, respectively. When accounting for the observed biases throughout the protein for negative pairwise epistasis and positive tertiary epistasis, the probabilities are both $<1.0 \times 10^{-6}$. This result substantiates the trend seen within smaller protein domains [18,19,50] (but see Lunzer *et al.* [15]).

Mutations in the interior of the protein (exposed surface area < 2%) were strongly biased to exhibit negative pairwise epistasis with G238S (Fig. 5d). Mutations in the core were also strongly biased to exhibit negative tertiary (Fig. 5e). Assuming the null hypothesis that positive and negative epistasis are equally probable in the core of the protein, the probability of observing biases at least this severe by chance were $<1.0 \times 10^{-6}$ and $<2.2 \times 10^{-6}$, respectively. When accounting for the observed biases throughout the protein for negative pairwise epistasis and positive tertiary epistasis, the probabilities change to $<5.3 \times 10^{-3}$ and $<1.0 \times 10^{-6}$,

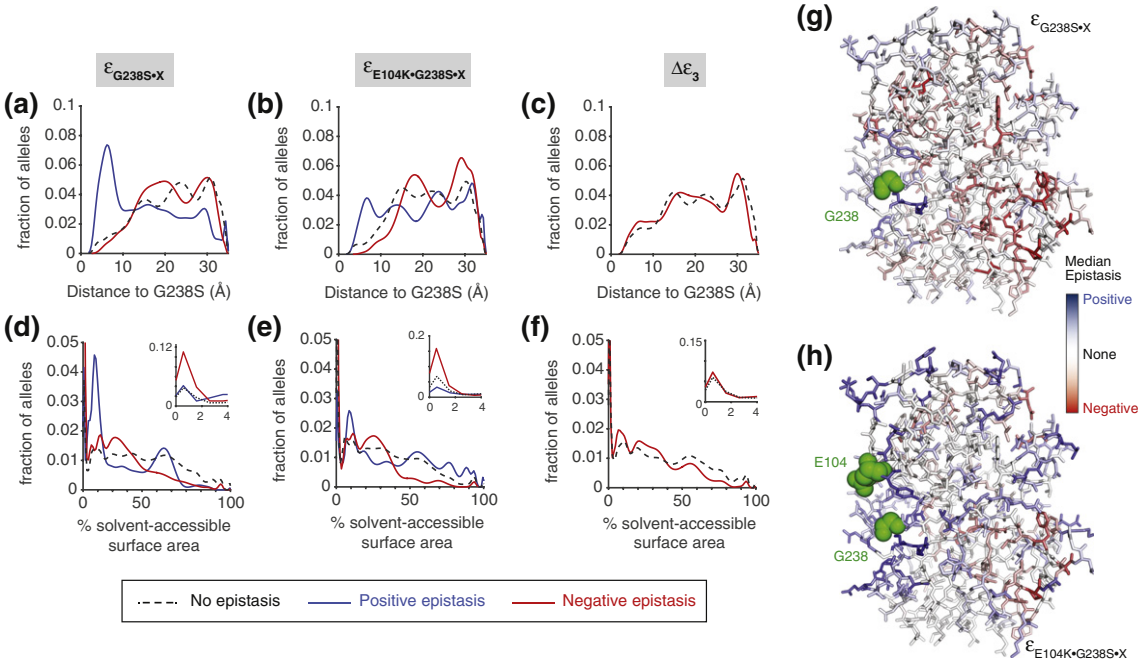

Fig. 5. The relationship between epistasis and protein structure. (a–c) The relationship between C-alpha distance from G238 to X and epistasis. (d–f) The relationship between solvent-accessible surface area of residue X and epistasis. (g, h) Median epistasis values mapped by color-coding onto the structure of TEM-1. Median values were calculated only for those positions for which epistasis values were measured for five or more mutations at that position. White can indicate no epistasis or insufficient data to calculate a median value. (a, d) depicts pairwise epistasis between G238S and X; (b, e) depicts tertiary epistasis among G238S, E104K, and X; and (c, f) indicates $\Delta\varepsilon_3$, the change in epistasis upon adding a third mutation. The number of positions with significant positive $\Delta\varepsilon_3$ was too small for analysis. Boxcar smoothing was applied to the data in (a–f) to aid visualization of the trends.

respectively. This prevalence for negative pairwise and tertiary epistasis involving G238S and core residues fits the threshold robustness model [5,39,40], as G238S and most core mutations are likely destabilizing mutations. Although there is evidence for coevolution of neutral surface mutations and deleterious core mutations with positive epistasis [51], highly exposed surface residues and G238S tend not to exhibit any pairwise epistasis (Fig. 5d and g). We postulate that the high frequency of positive tertiary epistasis involving surface mutations (Fig. 5h**)** merely results from the fact that these residues are more likely to be neutral mutations and thus less likely to disrupt the positive epistasis between E104K and G238S. Mutations that negatively affected the positive epistasis between E104K and G238S had a strong bias to be buried in the structure (Fig. 5f). To some extent, residues participating in positive epistasis tended to localize with other residues participating in positive epistasis, and residues participating in negative epistasis localized analogously (Fig. 5g and h, and 6e).

Given the localization of positive and negative epistasis in the structure of the protein, it is not too surprising that there was also localization in the primary sequence (Fig. 6). Positions 243 and 244 were prone to exhibit strong positive epistasis with G238S, most likely because these positions cooperatively provide stability with G238. Mutations in regions 161–167, 221–231, and the N- and C-termini of the protein (26, 29, 287, and 289) were prone to exhibit strong negative epistasis with G238S. Residues 161–167 compose the first third of the Ω-loop, which plays an important role in TEM-1's catalytic activity and specificity. Positions 221–231 comprise the end of a beta strand, a short alpha helix, and a loop that connects these two interacting structures. The residues at the N- and C-termini include interacting histidines H26 and H289, which help tie down the end of the two alpha helices that comprise the N- and C-termini of the protein, and I286, which forms a favorable interaction with P226 (i.e., a residue in the aforementioned 221–231 segment). We propose that mutations in these regions (221–231 and the N- and C-termini) and, in general, the core of the protein tend to have moderate destabilizing effects, but together with G238S, they exhaust the inherent stability buffer of the protein, resulting in negative pairwise epistasis with G238S.

Epistasis between the signal sequence and the protein

The first 23 codons of *TEM-1* encode the signal sequence that directs the protein to the periplasmic space of *E. coli*, where the signal sequence is removed. Although the signal sequence is not part of the mature protein, mutations therein can affect fitness by changing protein abundance as a result of codon usage effects at the beginning of the gene and alterations in export efficiency [33]. We wondered if epistasis could manifest between mutations in the signal sequence and the E104K/G238S mutations in the mature protein. We found that the means for $\varepsilon_{E104K•X}$ (0.00 ± 0.28), $\varepsilon_{G238S•X}$ (0.19 ± 0.28), and $\varepsilon_{E104K•G238S•X}$ (0.41 ± 0.23) for signal sequence mutations were statistically different from each other when compared pairwise ($p < 0.0001$ for all pairs, Student's *t*-test). Although $\varepsilon_{G238S•X}$ values for the mature protein tended toward negative epistasis, $\varepsilon_{G238S•X}$ values for the signal sequence tended toward positive epistasis (Fig. 6b), especially for signal sequence mutations with a negative effect on fitness in TEM-1. Since most signal sequence mutations are neutral or deleterious in TEM-1, this trend could reflect G238S's suspected capacity to cause protein aggregation [31] and the complex relationship between export rates and protein abundance. Decreased protein synthesis rates (and, analogously, export rates) can counterintuitively increase soluble protein levels by decreasing off-pathway aggregation [52]. Thus, mutations causing decreased protein translation or export might decrease aggregation, thereby increasing protein abundance, resulting in positive epistasis. The Q6R and H7R signal sequence mutations in TEM-1 increase both Amp resistance and protein abundance when the gene is on a higher copy number plasmid and under a stronger promoter than those used in our study [53]. The mechanism for these two mutation's beneficial effects was not determined, but the authors reasonably proposed that the mutations facilitated export to the periplasm. However, in our experiment, these mutations were not beneficial ($w_{Q6R} = 1.03 \pm 0.07$) and $w_{H7R} = 0.58 \pm 0.06$) and exhibited no epistasis with G238S, which indicates that these mutations have different effects in different contexts. The mean tertiary epistasis for signal sequence mutations matched $\varepsilon_{E104K•G238S}$ (0.40) (Fig. 6c), suggesting that for the most part, tertiary epistasis involving signal sequence mutations was positive only because the mutations did not affect the positive pairwise epistasis between E104K and G238S.

Sign epistasis along an evolutionary pathway

We further wanted to examine the changes in beneficial mutations between landscapes as caused by adaptation. The addition or removal of accessible advantageous mutations due to genetic background is termed sign epistasis [54]. Sign epistasis reflects the direct change in potential, advantageous evolutionary pathways between genetic backgrounds. Here, we count a mutation X as exhibiting sign epistasis if it is advantageous in one allele and disadvantageous in a second allele that differs from the first by only one amino acid substitution. Positive sign epistasis

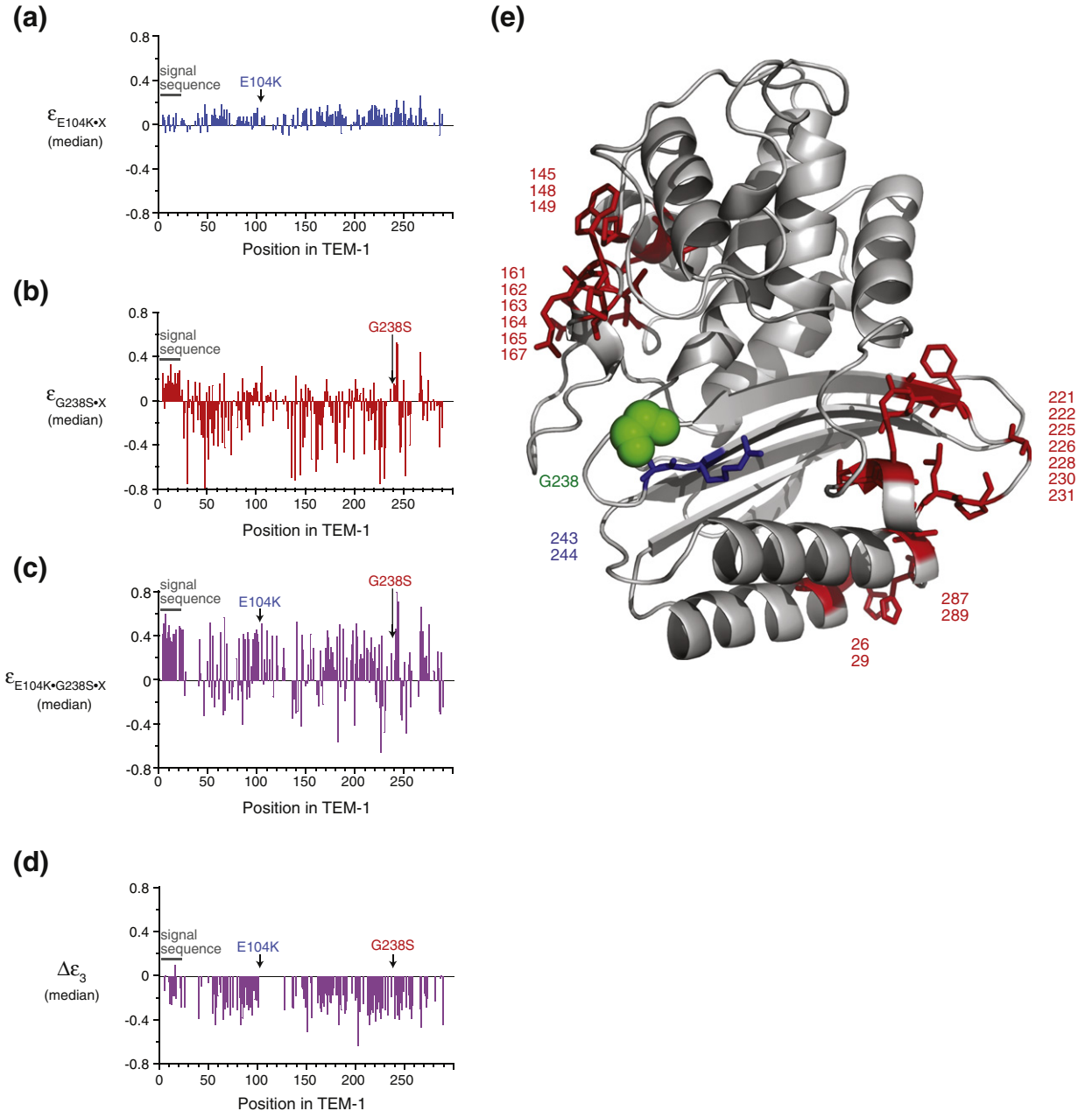

Fig. 6. Epistasis as a function of sequence and structure. (a–d) Median epistasis as a function of position in TEM-1 (using the Ambler consensus number scheme). Median values were calculated only for those positions for which epistasis values were measured for five or more mutations at that position. The lack of a bar can indicate no epistasis but usually means insufficient data to calculate a median value. (e) Selected regions in the structure of TEM-1 showing a tendency for positive (blue) or negative (red) epistasis with G238S, as defined by the median epistasis value. The numbers of the positions highlighted are indicated.

occurs when the mutation switches from deleterious to advantageous by the addition of an adaptive mutation (E104K or G238S). Negative sign epistasis is the inverse case. Our analysis indicates that the second adaptive mutation significantly increases the prevalence of negative sign epistasis (Fig. 7a). Mutations that are detrimental in TEM-1 but beneficial in TEM-19 have a higher frequency near G238S, especially at R241 and S243, and in the signal sequence (Supplementary Fig. S4a–d). The Ω-loop (160–178) is a hot spot for mutations exhibiting negative sign epistasis, with a relatively high occurrence of mutations that are

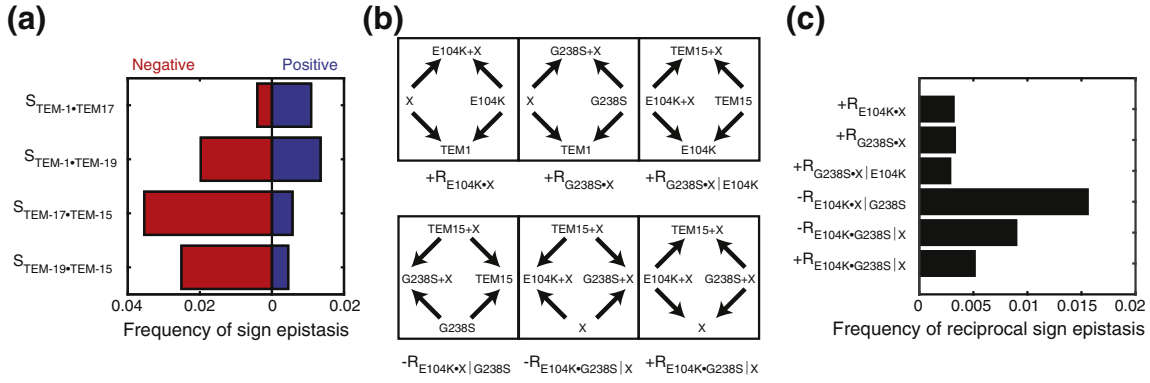

Fig. 7. Frequency of sign epistasis and ruggedness along an evolutionary pathway. (a) Frequency of sign epistasis, *S*, observed between alleles. Sign epistasis is defined as the switch from a mutation X being deleterious to beneficial (positive, blue) or from beneficial to deleterious (negative, red) by the addition of an adaptive mutation (E104K or G238S). For example, $S_{TEM-1•TEM-17}$ is positive if a mutation X was deleterious in TEM-1 but advantageous in TEM-17 (i.e., in the presence of E104K). (b) Illustration of all possible cases of reciprocal sign epistasis, *R*, among fitness landscapes analyzed. Arrows point toward increasing fitness between two alleles. (c) Fraction of sites demonstrating positive (+) and negative (–) reciprocal sign epistasis between landscapes. Terms are as defined in (b). Supplementary Data S2 tabulates all occurrences of sign and reciprocal sign epistasis.

advantageous in TEM-17 but deleterious in TEM-15 (Supplementary Fig. S4a–d). Apparently, E104K's deleterious effect on Amp resistance can be compensated for by these mutations in the nearby Ω-loop but not in the context of G238S. The overall loss of potential adaptive pathways indicated by the prevalence of negative sign epistasis is a cost of adaptation. Increasing magnitude and sign epistasis both support a fitness territory trade-off for the protein during adaptation.

Reciprocal sign epistasis and ruggedness along an evolutionary pathway

Reciprocal sign epistasis is a specialized case of sign epistasis in which multiple fitness peaks exist between alleles (Fig. 7b) [54]. This term is a direct measure of ruggedness between genetic backgrounds. As with sign epistasis, negative reciprocal sign epistasis occurs more frequently when both G238S and E104K are present (Fig. 7c). We find that 4.2% of the pathways are rugged between TEM-1 to TEM-15 + X (i.e., the pathways exhibit reciprocal sign epistasis). G238S is the primary cause of this ruggedness. Most of these rugged pathways (83%) include G238S + X as a local maximum, and the frequency of reciprocal sign epistasis is the highest near the G238S mutation (Supplementary Fig. S4e–f). We speculate that threshold robustness, by advantageously allowing for adaptive mutations that compromise protein stability, will generally lead to increased epistasis and landscape ruggedness along adaptive pathways. Ruggedness, as quantified here, represents potential evolutionary traps as local maxima are increased, potentially preventing adaptive pathways from reaching fitter maxima.

Conclusions

Our high-throughput, systematic approach to characterizing local fitness landscapes along an evolutionary pathway provides extensive maps of fitness and epistasis that reveal the consequences of adaptation for the original protein function in unprecedented detail. Adaptation moves the protein to an area of the fitness landscape that is characterized by decreased mutational robustness, increased frequency of epistasis (particularly negative epistasis), and increased ruggedness. For the adapted protein, deleterious mutations tend to be more deleterious, and the synergistic effects of beneficial mutations begin to erode. All these consequences represent a cost of adaptation that we term a fitness territory trade-off. To a large extent, this trade-off results from the destabilizing effects of the G238S mutation (an adaptive mutation that fits the function–stability trade-off principle) that tends to exhibit negative pairwise epistasis with other mutations, in accord with the threshold robustness model. Thus, the fitness territory trade-off results from G238S's destabilizing nature rather than its adaptive nature for cefotaxime resistance per se. A residue's statistical preferences for epistatic effects can be partially understood in terms of structural models. In addition, the extent of a mutation's effect showed statistical preferences for the type of epistasis. Whereas moderately deleterious mutations tend to exhibit negative epistasis, severely deleterious mutations were equally likely to exhibit positive or negative epistasis. We propose an explanation for these observations involving the threshold robustness model coupled with a mechanistic understanding of the origin of the severely deleterious effects.

Materials and Methods

Mutagenesis

Comprehensive saturation mutagenesis of *TEM-17*, *TEM-19*, and *TEM-15* was performed as previously described for *TEM-1* [34]. Mutagenic oligonucleotides containing the degenerate codon NNN were targeted to every codon of the genes. We designed the process to create a library consisting of all 19 × 286 = 5434 mutants that differ from the template gene by only one amino acid substitution.

Selection

Selection was performed using the band-pass genetic circuit described previously [33] with the following exceptions. We used plasmid pTS40 instead of pTS42. Plasmid pTS42 is identical to pTS40 except that a small section of inconsequential DNA between the chloramphenicol resistance gene and the *CloDF13* has been removed. We used 10 μg/ml tetracycline in the band-pass selection experiments with cefotaxime. Ampicillin selections spanned 13 plates doubling in concentration from 0.25 μg/ml to 1024 μg/ml Amp, while cefotaxime selections spanned seven plates doubling from 0.01 μg/ml to 0.64 μg/ml cefotaxime. We measured the frequency of colonies appearing on each plate (in triplicate), in order to send the subsequently prepared amplicons to sequencing in the right proportion that properly reflects every allele frequency in the whole library. For example, if plate 1 had twice the number of colonies as plate 2, the amount of DNA sent for sequencing from plate 1 was twice as that from plate 2.

Deep sequencing

Deep sequencing was performed using amplicons generated from plasmid DNA isolated from each swept selection plate as described [33]. In this study, however, 3 bp barcodes indicating the plate were added on each side of the amplicon to identify the plate from which the amplicon originated. PacBio deep sequencing was performed on these amplicons and analyzed using a three-pass circular consensus criterion.

Data analysis

We used custom Matlab scripts to align, analyze, and quantify reads and amino acid mutation composition (synonymous codons were grouped together). Reads were filtered for quality score (reported average quality score >30, or average reported probability of error = 10^{-3}), length (length of read less than 1100 bp but more than 930 bp), and quality of alignment to the reference gene (entirety of reference gene aligned to read) and the barcode (perfect match accepted only). If insertions or deletions were encountered within 3 bp of a substitution, the read was discarded due to possible misalignment of a mutation and ambiguity of position. Other cases of insertions and deletions were assumed to be sequencing errors. Each read was then aligned to the reference gene, as well as each barcode, to identify and catalog mutations. Only reads with a full alignment to the reference and only containing one codon substitution were accepted for analysis.

To calculate fitness values, we tabulated the number of sequencing reads (the counts) for each allele at each Amp or cefotaxime concentration (S3–6 Data). We identified the plate with the highest adjusted counts for each allele, set a window including the two plates on either side (five total), and determined the fitness using the counts from these five plates, as described previously [33] with one minor difference. In our previous work, the counts were used directly in the calculation. Here, we adjusted the counts to reflect the desired proportion of amplicons from each plate as determined by the frequency of colonies appearing on that plate. For example, if the frequency of reads of amplicons coming from plate 3 in the deep sequencing was 50% higher than the frequency of colonies appearing on plate 3, we reduced the counts of alleles on plate 3 by dividing by 1.5. We also applied this adjustment to the previously published fitness measurements of TEM-1 [33], resulting in minor changes in the fitness values.

The method of calculating fitness is described in more detail in Ref. [33] and is briefly summarized here. The unnormalized fitness value f of mutant allele (i) is calculated by averaging the number of reads from each plate (p) using the following equation, where c represents the number of PacBio read counts and a represents the concentration of Amp on plate (p) in μg/ml (as identified from the DNA barcode):

$$f_{\mathrm{i}} = \frac{\sum_{\mathrm{p}=1}^{13} c_{\mathrm{i,p}}\, log_2(a_{\mathrm{p}})}{\sum_{\mathrm{p}=1}^{13} c_{\mathrm{i,p}}} \tag{6}$$

The unnormalized fitness f represents the resistance of each mutant to Amp. It is the $\log_2$ of the concentration of Amp that is the center of the counts. We determined the normalized fitness w_{i} relative to the fitness of TEM-1 using Eq (7).

$$w_{\mathrm{i}} = \frac{2^{f_{\mathrm{i}}}}{2^{f_{\mathrm{TEM-1}}}} \tag{7}$$

The normalized fitness (w) is unitless and represents the fraction of antibiotic resistance conferred relative to that conferred by *TEM-1*. Except where noted, all fitness values are relative to TEM-1, which was set to a fitness value of 1.00.

In cases of finding two clusters of counts for an allele (using K-means clustering), preference was given to the cluster containing more than one synonymous codon. A fitness peak was determined iteratively: if a window around the plate with the highest number of counts did not contain five counts, the next peak was found and evaluated. In this way, only alleles with five or more counts (before adjustment) were considered.

We determined an upper-level estimate of the fractional error in fitness (e_{w}) using Eq (8), which is our previously determined correlation between the total sequencing counts of an allele (n) and the standard deviation of the difference in fitness among synonymous alleles [33].

$$e_{\mathrm{w}} = 0.667 n^{-0.387} \tag{8}$$

The error in fitness σ_w is found by multiplying e_w by the fitness value w. The number of counts of TEM-1, TEM-17, TEM-19, and TEM-15 exceeded the range of counts in the data used to determine the correlation of Eq (8). Thus, for these four fitness values, we conservatively assumed a fractional error of 0.10, although we expect the error to be less.

Epistasis values were calculated using Eqs. (1) and (3). The upper and lower limits on the pairwise epistasis values were determined using Eqs. (9) and (10), respectively. The uncertainty in the tertiary epistasis values were determined analogously using Eqs. (11) and (12). The uncertainty in $\Delta\varepsilon_3$ was determined using Eqs. (13) and (14).

$$\varepsilon_{AB,U} = log_{10}\left[\frac{w_{AB}w_0}{w_A w_B}\left(1+\sqrt{e_A{}^2+e_B{}^2+e_0{}^2+e_{AB}{}^2}\right)\right] \quad (9)$$

$$\varepsilon_{AB,L} = log_{10}\left[\frac{w_{AB}w_0}{w_A w_B}\left(1-\sqrt{e_A{}^2+e_B{}^2+e_0{}^2+e_{AB}{}^2}\right)\right] \quad (10)$$

$$\varepsilon_{ABX,U} = log_{10}\left[\frac{w_{ABX}w_0{}^2}{w_A w_B w_X} \times\left(1+\sqrt{e_A{}^2+e_B{}^2+e_X{}^2+2e_0{}^2+e_{ABX}{}^2}\right)\right] \quad (11)$$

$$\varepsilon_{ABX,L} = log_{10}\left[\frac{w_{ABX}w_0{}^2}{w_A w_B w_X} \times\left(1-\sqrt{e_A{}^2+e_B{}^2+e_X{}^2+2e_0{}^2+e_{ABX}{}^2}\right)\right] \quad (12)$$

$$\Delta\varepsilon_{3,U} = \log_{10}\left[\frac{w_{ABX}w_x w_A w_B}{w_{AX}w_{BX}w_{AB}w_0} \times\left(1+\sqrt{e_A{}^2+e_B{}^2+e_X{}^2+e_0{}^2+e_{AX}{}^2+e_{BX}{}^2+e_{AB}{}^2+e_{ABX}{}^2}\right)\right] \quad (13)$$

$$\Delta\varepsilon_{3,L} = \log_{10}\left[\frac{w_{ABX}w_x w_A w_B}{w_{AX}w_{BX}w_{AB}w_0} \times\left(1-\sqrt{e_A{}^2+e_B{}^2+e_X{}^2+e_0{}^2+e_{AX}{}^2+e_{BX}{}^2+e_{AB}{}^2+e_{ABX}{}^2}\right)\right] \quad (14)$$

In Fig. 1, the criteria for a significant difference in the effect of the mutation in the two genetic backgrounds was that the two fitness values (normalized to their respective genetic backgrounds) differed by more than twice the sum of the errors in fitness. In Fig. 3, the criteria for mutations to be designated as exhibiting significant positive and negative epistasis determined by Eqs. (15) and (16), respectively. Significance requires that the epistasis value (or $\Delta\varepsilon_3$ value) be different from zero assuming the uncertainty is twice that calculated.

$$\varepsilon - 2(\varepsilon - \epsilon_L) > 0 \quad (15)$$

$$\varepsilon - 2(\varepsilon - \epsilon_U) < 0 \quad (16)$$

Sign epistasis was determined solely by fitness measurements [55]. In this case, sign epistasis of a mutation X between alleles A and B was counted as positive (+1) if the fitness of X in the background of A was significantly detrimental (fitness w_{XA} was less than the wild-type value w_A minus twice the fitness error), while the fitness of X in the background of B was significantly advantageous (fitness w_{XB} was greater than the wild-type value w_B plus twice the fitness error). Negative sign epistasis (−1) is the inverse of this case. The frequency of sign epistasis between alleles A and B, $S_{A\bullet B}$, was found by summing all occurrences of sign epistasis and dividing by the size of the total data set. The criteria for reciprocal sign epistasis, $R_{A\bullet B}$, incorporated identical error calculation but was further specified by the cases illustrated in Fig. 7b. $R_{A\bullet B}$ was defined as positive (+1) if the combination of mutations A and B constituted a local maximum (synergistic effect). Negative $R_{A\bullet B}$(−1) is the inverse case (antagonistic effect).

Acknowledgments

This research was supported by the National Science Foundation (grant numbers DEB-0950939, DEB-1353143, and CBET-1402101 to M.O.).

Author contributions: B.S. performed the experiments, and B.S. and M.O. conceived and designed the experiments, analyzed the data, and wrote the paper.

Appendix A. Supplementary data

Supplementary data to this article can be found online at http://dx.doi.org/10.1016/j.jmb.2016.04.033.

Received 1 February 2016;
Received in revised form 18 April 2016;
Accepted 29 April 2016
Available online 10 May 2016

Keywords:
protein evolution;
epistasis;
beta-lactamase;
fitness landscape

Current address: B. Steinberg, Editas Medicine, 300 Third Street, First Floor, Cambridge, MA 02142 USA.

Abbreviations used:
β-lactamases, beta-lactamases; β-lactam, beta-lactam; Amp, Amp; MIC, minimum inhibitory concentration.

References

[1] A. Matagne, J. Lamotte-Brasseur, J.M. Frere, Catalytic properties of class A beta-lactamases: efficiency and diversity, Biochem. J. 330 (Pt 2) (1998) 581–598.

[2] M.F. Schenk, S. Witte, M.L.M. Salverda, B. Koopmanschap, J. Krug, J.A.G.M. Visser, Role of pleiotropy during adaptation of *TEM-1* β-lactamase to two novel antibiotics, Evol. Appl. 8 (2014) 248–260, http://dx.doi.org/10.1111/eva.12200.

[3] V.A. Risso, J.A. Gavira, D.F. Mejia-Carmona, E.A. Gaucher, J.M. Sanchez-Ruiz, Hyperstability and substrate promiscuity in laboratory resurrections of precambrian β-lactamases, ACS Synth. Biol. 135 (2013) 2899–2902, http://dx.doi.org/10.1021/ja311630a.
[4] S. Bershtein, K. Goldin, D.S. Tawfik, Intense neutral drifts yield robust and evolvable consensus proteins, J. Mol. Biol. 379 (2008) 1029–1044, http://dx.doi.org/10.1016/j.jmb.2008.04.024.
[5] S. Bershtein, M. Segal, R. Bekerman, N. Tokuriki, D.S. Tawfik, Robustness-epistasis link shapes the fitness landscape of a randomly drifting protein, Nature 444 (2006) 929–932, http://dx.doi.org/10.1038/nature05385.
[6] J.D. Bloom, P.A. Romero, Z. Lu, F.H. Arnold, Neutral genetic drift can alter promiscuous protein functions, potentially aiding functional evolution, Biol. Direct 2 (2007) 17, http://dx.doi.org/10.1186/1745-6150-2-17.
[7] J.I. Boucher, P. Cote, J. Flynn, L. Jiang, A. Laban, P. Mishra, et al., Viewing protein fitness landscapes through a next-gen lens, Genetics 198 (2014) 461–471, http://dx.doi.org/10.1534/genetics.114.168351.
[8] D.M. Fowler, S. Fields, Deep mutational scanning: a new style of protein science, Nat. Methods 11 (2014) 801–807, http://dx.doi.org/10.1038/nmeth.3027.
[9] S. Gavrilets, Fitness Landscapes and the Origin of Species, Princeton University Press, Princeton, NJ, 2004.
[10] P.C. Phillips, Epistasis—the essential role of gene interactions in the structure and evolution of genetic systems, Nat. Rev. Genet. 9 (2008) 855–867, http://dx.doi.org/10.1038/nrg2452.
[11] D.J. Kvitek, G. Sherlock, Reciprocal sign epistasis between frequently experimentally evolved adaptive mutations causes a rugged fitness landscape, PLoS Genet. 7 (2011), e1002056, http://dx.doi.org/10.1371/journal.pgen.1002056.
[12] D.A. Kondrashov, F.A. Kondrashov, Topological features of rugged fitness landscapes in sequence space, Trends Genet. 31 (2015) 24–33, http://dx.doi.org/10.1016/j.tig.2014.09.009.
[13] G. Martin, S.F. Elena, T. Lenormand, Distributions of epistasis in microbes fit predictions from a fitness landscape model, Nat. Genet. 39 (2007) 555–560, http://dx.doi.org/10.1038/ng1998.
[14] L.I. Gong, J.D. Bloom, Epistatically interacting substitutions are enriched during adaptive protein evolution, PLoS Genet. 10 (2014), e1004328, http://dx.doi.org/10.1371/journal.pgen.1004328.
[15] M. Lunzer, G.B. Golding, A.M. Dean, Pervasive cryptic epistasis in molecular evolution, PLoS Genet. 6 (2010) e1001162, http://dx.doi.org/10.1371/journal.pgen.1001162.
[16] J.A. Draghi, J.B. Plotkin, Selection biases the prevalence and type of epistasis along adaptive trajectories, Evolution 67 (2013) 3120–3131, http://dx.doi.org/10.1111/evo.12192.
[17] D. Greene, K. Crona, The changing geometry of a fitness landscape along an adaptive walk, PLoS Comput. Biol. 10 (2014), e1003520http://dx.doi.org/10.1371/journal.pcbi.1003520.
[18] D. Melamed, D.L. Young, C.E. Gamble, C.R. Miller, S. Fields, Deep mutational scanning of an RRM domain of the *Saccharomyces cerevisiae* poly(A)-binding protein, RNA 19 (2013) 1537–1551, http://dx.doi.org/10.1261/rna.040709.113.
[19] C.A. Olson, N.C. Wu, R. Sun, A comprehensive biophysical description of pairwise epistasis throughout an entire protein domain, Curr. Biol. (2014) 2643–2651, http://dx.doi.org/10.1016/j.cub.2014.09.072.
[20] C.L. Araya, D.M. Fowler, Deep mutational scanning: assessing protein function on a massive scale, Trends Biotechnol. (2011) 435–442, http://dx.doi.org/10.1016/j.tibtech.2011.04.003.
[21] C. Bank, R.T. Hietpas, J.D. Jensen, D.N.A. Bolon, A systematic survey of an intragenic epistatic landscape, Mol. Biol. Evol. 32 (2014) 229–238, http://dx.doi.org/10.1093/molbev/msu301.
[22] H. Jacquier, A. Birgy, H. Le Nagard, Y. Mechulam, E. Schmitt, J. Glodt, et al., Capturing the mutational landscape of the beta-lactamase TEM-1, Proc. Natl. Acad. Sci. 110 (2013) 13,067–13,072, http://dx.doi.org/10.1073/pnas.1215206110.
[23] A.I. Podgornaia, M.T. Laub, Pervasive degeneracy and epistasis in a protein–protein interface, Science 347 (2015) 673–677, http://dx.doi.org/10.1126/science.1257360.
[24] T. Hinkley, J. Martins, C. Chappey, M. Haddad, E. Stawiski, J.M. Whitcomb, et al., A systems analysis of mutational effects in HIV-1 protease and reverse transcriptase, Nat. Genet. 43 (2011) 487–489, http://dx.doi.org/10.1038/ng.795.
[25] J. Otwinowski, J.B. Plotkin, Inferring fitness landscapes by regression produces biased estimates of epistasis, Proc. Natl. Acad. Sci. 111 (2014) E2301–E2309, http://dx.doi.org/10.1073/pnas.1400849111.
[26] C. Mabilat, P. Courvalin, Development of "oligotyping" for characterization and molecular epidemiology of TEM beta-lactamases in members of the family Enterobacteriaceae, Antimicrob. Agents Chemother. 34 (1990) 2210–2216, http://dx.doi.org/10.1128/AAC.34.11.2210.
[27] B.G. Hall, Predicting evolution by *in vitro* evolution requires determining evolutionary pathways, Antimicrob. Agents Chemother. 46 (2002) 3035–3038, http://dx.doi.org/10.1128/AAC.46.9.3035-3038.2002.
[28] X. Wang, G. Minasov, B.K. Shoichet, Evolution of an antibiotic resistance enzyme constrained by stability and activity trade-offs, J. Mol. Biol. 320 (2002) 85–95, http://dx.doi.org/10.1016/S0022-2836(02)00400-X.
[29] X. Raquet, M. Vanhove, J. Lamotte-Brasseur, S. Goussard, P. Courvalin, J.M. Frere, Stability of TEM beta-lactamase mutants hydrolyzing third generation cephalosporins, Proteins 23 (1995) 63–72, http://dx.doi.org/10.1002/prot.340230108.
[30] C. Cantu, T. Palzkill, The role of residue 238 of TEM-1 beta-lactamase in the hydrolysis of extended-spectrum antibiotics, J. Biol. Chem. 273 (1998) 26,603–26,609, http://dx.doi.org/10.1074/jbc.273.41.26603.
[31] D.M. Weinreich, N.F. Delaney, M.A. Depristo, D.L. Hartl, Darwinian evolution can follow only very few mutational paths to fitter proteins, Science 312 (2006) 111–114, http://dx.doi.org/10.1126/science.1123539.
[32] M.A. Stiffler, D.R. Hekstra, R. Ranganathan, Evolvability as a function of purifying selection in *TEM-1* β-lactamase, Cell 160 (2015) 882–892, http://dx.doi.org/10.1016/j.cell.2015.01.035.
[33] E. Firnberg, J.W. Labonte, J.J. Gray, M. Ostermeier, A comprehensive, high-resolution map of a gene's fitness landscape, Mol. Biol. Evol. 31 (2014) 1581–1592, http://dx.doi.org/10.1093/molbev/msu081.
[34] E. Firnberg, M. Ostermeier, PFunkel: efficient, expansive, user-defined mutagenesis, PLoS ONE 7 (2012) e52031, http://dx.doi.org/10.1371/journal.pone.0052031.
[35] T. Sohka, R.A. Heins, R.M. Phelan, J.M. Greisler, C.A. Townsend, M. Ostermeier, An externally tunable bacterial band-pass filter, Proc. Natl. Acad. Sci. 106 (2009) 10,135–10,140, http://dx.doi.org/10.1073/Pnas.0901246106.
[36] S. Bershtein, D.S. Tawfik, Ohno's model revisited: measuring the frequency of potentially adaptive mutations under various

mutational drifts, Mol. Biol. Evol. 25 (2008) 2311–2318, http://dx.doi.org/10.1093/molbev/msn174.
[37] B. Østman, A. Hintze, C. Adami, Impact of epistasis and pleiotropy on evolutionary adaptation, Proc. Biol. Sci. 279 (2012) 247–256, http://dx.doi.org/10.1098/rspb.2011.0870.
[38] D. Berger, E. Postma, Biased estimates of diminishing-returns epistasis? empirical evidence revisited, Genetics 198 (2014) 1417–1420, http://dx.doi.org/10.1534/genetics.114.169870.
[39] J.D. Bloom, J.J. Silberg, C.O. Wilke, D.A. Drummond, C. Adami, F.H. Arnold, Thermodynamic prediction of protein neutrality, Proc. Natl. Acad. Sci. 102 (2005) 606–611, http://dx.doi.org/10.1073/pnas.0406744102.
[40] N. Tokuriki, D.S. Tawfik, Stability effects of mutations and protein evolvability, Curr. Opin. Struct. Biol. 19 (2009) 596–604, http://dx.doi.org/10.1016/j.sbi.2009.08.003.
[41] J. da Silva, M. Coetzer, R. Nedellec, C. Pastore, D.E. Mosier, Fitness epistasis and constraints on adaptation in a human immunodeficiency virus type 1 protein region, Genetics 185 (2010) 293–303, http://dx.doi.org/10.1534/genetics.109.112458.
[42] L. Tan, S. Serene, H. Chao, J. Gore, Hidden randomness between fitness landscapes limits reverse evolution, Phys. Rev. Lett. 106 (2011) http://dx.doi.org/10.1103/PhysRevLett.106.198102.
[43] Q.K. Thai, F. Bös, J. Pleiss, The lactamase engineering database: a critical survey of TEM sequences in public databases, BMC Genomics 10 (2009) 390, http://dx.doi.org/10.1186/1471-2164-10-390.
[44] M. Barlow, B.G. Hall, Predicting evolutionary potential: *in vitro* evolution accurately reproduces natural evolution of the TEM beta-lactamase, Genetics 160 (2002) 823–832.
[45] G. Kopsidas, R.K. Carman, E.L. Stutt, A. Raicevic, A.S. Roberts, M.-A.V. Siomos, et al., RNA mutagenesis yields highly diverse mRNA libraries for *in vitro* protein evolution, BMC Biotechnol. 7 (2007) 18, http://dx.doi.org/10.1186/1472-6750-7-18.
[46] M.C. Orencia, J.S. Yoon, J.E. Ness, W.P. Stemmer, R.C. Stevens, Predicting the emergence of antibiotic resistance by directed evolution and structural analysis, Nat. Struct. Biol. 8 (2001) 238–242, http://dx.doi.org/10.1038/84981.
[47] W.P. Stemmer, Rapid evolution of a protein *in vitro* by DNA shuffling, Nature 370 (1994) 389–391, http://dx.doi.org/10.1038/370389a0.
[48] M. Zaccolo, E. Gherardi, The effect of high-frequency random mutagenesis on *in vitro* protein evolution: a study on TEM-1 beta-lactamase, J. Mol. Biol. 285 (1999) 775–783, http://dx.doi.org/10.1006/jmbi.1998.2262.
[49] M.L.M. Salverda, E. Dellus, F.A. Gorter, A.J.M. Debets, J. van der Oost, R.F. Hoekstra, et al., Initial mutations direct alternative pathways of protein evolution, PLoS Genet. 7 (2011), e1001321, http://dx.doi.org/10.1371/journal.pgen.1001321.
[50] A.F.Y. Poon, L. Chao, Functional origins of fitness effect-sizes of compensatory mutations in the DNA bacteriophage phiX174, Evolution 60 (2006) 2032–2043, http://dx.doi.org/10.1111/j.0014-3820.2006.tb01841.x.
[51] A. Toth-Petroczy, D.S. Tawfik, Slow protein evolutionary rates are dictated by surface–core association, Proc. Natl. Acad. Sci. 108 (2011) 11,151–11,156, http://dx.doi.org/10.1073/pnas.1015994108.
[52] F. Baneyx, M. Mujacic, Recombinant protein folding and misfolding in *Escherichia coli*, Nat. Biotechnol. 22 (2004) 1399–1408, http://dx.doi.org/10.1038/nbt1029.
[53] M. Goldsmith, D.S. Tawfik, Potential role of phenotypic mutations in the evolution of protein expression and stability, Proc. Natl. Acad. Sci. 106 (2009) 6197–6202, http://dx.doi.org/10.1073/pnas.0809506106.
[54] F.J. Poelwijk, D.J. Kiviet, D.M. Weinreich, S.J. Tans, Empirical fitness landscapes reveal accessible evolutionary paths, Nature 445 (2007) 383–386, http://dx.doi.org/10.1038/nature05451.
[55] F.J. Poelwijk, S. Tănase-Nicola, D.J. Kiviet, S.J. Tans, Reciprocal sign epistasis is a necessary condition for multi-peaked fitness landscapes, J. Theor. Biol. 272 (2011) 141–144, http://dx.doi.org/10.1016/j.jtbi.2010.12.015.